

# Structural Mediation of Interlayer Excitation Transport in Zirconium–Phosphonate Multilayers

J. C. Horne and G. J. Blanchard\*

Contribution from the Michigan State University, Department of Chemistry,  
East Lansing, Michigan 48824-1322

Received July 20, 1998

**Abstract:** We report on our investigation of interlayer excitation transport in zirconium–phosphonate (ZP) multilayer structures. We find that dipolar (Förster) excitation transfer between energetically overlapped oligothiophene chromophores in adjacent layers does not play a significant role in determining the relaxation dynamics of these systems. This finding is not consistent with the predictions of the Förster model, and we account for this discrepancy by considering the spatial modulation of the dielectric response of the ZP multilayer assemblies. The presence of polarizable Zr–bis(phosphonate) layers between layers of donor and acceptor chromophores serves to screen dipolar D–A coupling. Intralayer excitation transfer within individual chromophore aggregates dominates population relaxation dynamics in these systems. We also find that spacing the chromophore-containing layers away from the primed substrate surface does not eliminate chromophore aggregation. We discuss these data in terms of the dominant factors in the formation of ZP layers.

## Introduction

Using molecular self-assembly to design novel interfaces is a promising research venue in materials science and in the development of nanoscale technologies. For such interfacial chemistry to realize its full potential, the ability to grow multiple layers in a controlled manner is essential. The synthesis of multiple, discrete layers using thiol and disulfide chemistry has not been investigated until recently,<sup>1</sup> and there remains much to be learned about this class of systems. Silane chemistry has been used for covalent multilayer growth,<sup>2–4</sup> but this chemistry can be difficult to control and it is susceptible to unwanted polymerization reactions, precluding the ability to create uniform, layered interfaces. The best approach devised to date for controlled multilayer growth is metal–phosphonate (MP) chemistry.<sup>5–21</sup> The extended MP structure that connects indi-

vidual layers is insoluble in most solvents, and the fact that there are two constituents (metal ion and phosphonate) allows for the controlled growth of individual layers; polymerization or spontaneous multilayer growth is precluded. The resulting multilayer structures are chemically and thermally robust, with the stability of the system being limited by the organobis-(phosphonate) layer constituents. Discrete layers can be built up using several different metal ions, Zr<sup>4+</sup> being the most common, and a wide variety of organophosphonates and organophosphates have been used. The combination of robustness and chemical versatility provides access to a wide range of film properties. These materials have been investigated for potential application in areas such as light harvesting, artificial photosynthesis, and optical information storage.<sup>7,15,16,22–24</sup>

The purpose of our work with metal–phosphonate multilayer structures is to understand excitation transport and the molecular-scale structural properties of these systems from a fundamental perspective. We investigate these multilayers with an eye toward their potential utility for reversible optical information storage. For optical information to be read and written, “on” and “off” conditions exhibiting different optical responses must be identified, and we are in the process of synthesizing molecules that satisfy this requirement.<sup>25</sup> Regardless of the chemical identity

\* To whom correspondence should be addressed.

(1) Kohli, P. K.; Harris, J. J.; Blanchard, G. J. *J. Am. Chem. Soc.* **1998**, *120*, 11962.

(2) Gun, J.; Iscovici, R.; Sagiv, J. *J. Colloid Interface Sci.* **1984**, *101*, 201.

(3) Maoz, R.; Sagiv, J. *J. Colloid Interface Sci.* **1984**, *100*, 465.

(4) Maoz, R.; Sagiv, J. *Thin Solid Films* **1985**, *132*, 135.

(5) Hong, H.-G.; Sackett, D. D.; Mallouk, T. E. *Chem. Mater.* **1991**, *3*, 521.

(6) Thompson, M. E. *Chem. Mater.* **1994**, *6*, 1168.

(7) Katz, H. E.; Wilson, W. L.; Scheller, G. *J. Am. Chem. Soc.* **1994**, *116*, 6636.

(8) Yonemoto, E. H.; Saupe, G. B.; Schmehl, R. H.; Hubig, S. M.; Riley, R. L.; Iverson, B. L.; Mallouk, T. E. *J. Am. Chem. Soc.* **1994**, *116*, 4786.

(9) Katz, H. E.; Bent, S. F.; Wilson, W. L.; Schilling, M. L.; Ungashe, S. B. *J. Am. Chem. Soc.* **1994**, *116*, 6631.

(10) Frey, B. L.; Hanken, D. G.; Corn, R. M. *Langmuir* **1993**, *9*, 1815.

(11) Yang, H. C.; Aoki, K.; Hong, H.-G.; Sackett, D. D.; Arendt, M. F.; Yau, S.-L.; Bell, C. M.; Mallouk, T. E. *J. Am. Chem. Soc.* **1993**, *115*, 11855.

(12) Vermeulen, L.; Thompson, M. E. *Nature* **1992**, *358*, 656.

(13) Ungashe, S. B.; Wilson, W. L.; Katz, H. E.; Scheller, G. R.; Putvinski, T. M. *J. Am. Chem. Soc.* **1992**, *114*, 8717.

(14) Cao, G.; Rabenberg, L. K.; Nunn, C. M.; Mallouk, T. M. *Chem. Mater.* **1991**, *3*, 149.

(15) Katz, H. E.; Schilling, M. L.; Chidsey, C. E. D.; Putvinski, T. M.; Hutton, R. S. *Chem. Mater.* **1991**, *3*, 699.

(16) Katz, H. E.; Scheller, G.; Putvinski, T. M.; Schilling, M. L.; Wilson, W. L.; Chidsey, C. E. D. *Science* **1991**, *254*, 1485.

(17) Putvinski, T. M.; Schilling, M. L.; Katz, H. E.; Chidsey, C. E. D.; Mujisce, A. M.; Emerson, A. B. *Langmuir* **1990**, *6*, 1567.

(18) Rong, D.; Hong, H.-G.; Kim, Y.-I.; Krueger, J. S.; Mayer, J. E.; Mallouk, T. E. *Coord. Chem. Rev.* **1990**, *97*, 237.

(19) Lee, H.; Kepley, L. J.; Hong, H.-G.; Akhter, S.; Mallouk, T. E. *J. Phys. Chem.* **1988**, *92*, 2597.

(20) Lee, H.; Kepley, L. J.; Hong, H.-G.; Mallouk, T. E. *J. Am. Chem. Soc.* **1988**, *110*, 618.

(21) Katz, H. E. *Chem. Mater.* **1994**, *6*, 2227.

(22) Vermeulen, L. A.; Snover, J. L.; Sapochak, L. S.; Thompson, M. E. *J. Am. Chem. Soc.* **1993**, *115*, 11767.

(23) Snover, J. L.; Byrd, H.; Suponeva, E. P.; Vicenzi, E.; Thompson, M. E. *Chem. Mater.* **1996**, *8*, 1490.

(24) Kaschak, D. M.; Mallouk, T. E. *J. Am. Chem. Soc.* **1996**, *118*, 4222.

(25) Delacruz, J. L.; Blanchard, G. J. In preparation.

of the information storing molecule, the switching between logical states will necessarily be mediated by an excited electronic state. Because of the requisite electronic excitation and the proximity of chromophores to one another, the issue of excitation transport must be considered in detail for these systems. Both interlayer and intralayer processes must be evaluated to understand the physical limits on the localization of excitations within multilayer assemblies. In the preceding paper we have considered intralayer excitation transport in detail and have found that aggregation and island formation dominates the structural and optical properties of individual layers.<sup>26</sup> With this understanding in place, we consider the efficiency of excitation transport between layers here. To understand and control excitation transport in MP films, we have constructed a series of chromophore-containing MP multilayer films where the spatial relationship between photon donors and acceptors is well-controlled.

To study excitation transport within and between individual molecular layers, chromophores with specific optical properties must be used. To facilitate excitation transport and thus place limits on the possible structural motifs appropriate for optical information storage in multilayer systems, the emission band of the donor should overlap the absorption band of the acceptor. The thiophene oligomers 2,2'-bithiophenediylbis(phosphonate) (BDP) and 2,2':5',5'':2'',2'''-quaterthiophenediylbis(phosphonate) (QDP) are the photon donor and acceptor chromophores, respectively. These are the same chromophores we used in the preceding paper. The emission band of BDP overlaps the absorption band of QDP. The thiophene oligomers are not candidates for optical information storage applications because of the facile rotation of individual thiophene rings within the chromophores.<sup>27</sup> This property is beneficial to this work because it precludes significant steric contributions to excitation transport.

In previous studies, we have focused on achieving a fundamental understanding of the chromophores both individually and in mixed monolayers.<sup>26,28,29</sup> We now know that the properties of the layers are mediated to a substantial extent by the silanol density and distribution on SiO<sub>x</sub> and oxidized Si surfaces. Silane-primed SiO<sub>x</sub> surfaces are characterized by islands, and the growth of at least the first several organophosphonate layers is templated by the chemically reactive islands.<sup>26,29</sup> Atomic force microscopy (AFM) images of the primed substrates and of monolayers have confirmed the presence of islands. In addition to the primer island formation, which is mediated by heterogeneity in the distribution of surface silanol sites, the oligothiophene chromophores aggregate during the deposition process, reinforcing the substrate-mediated island structure. Because of the dominant role of the aggregate islands within these monolayers and the interisland spacing, intralayer excitation transport over mesoscopic length scales is not efficient.<sup>26</sup>

This paper focuses on understanding excitation transport between different layers in systems where there is not a statistical distribution of donors and/or acceptors within individual layers. We have synthesized zirconium–phosphonate (ZP) multilayer structures with the donor and acceptor chromophores present in varying amounts in different layers. We expect and observe the same island morphology that we have elucidated previously for individual layers. We have found that excitation transport between the donor and acceptor chromophores across different

layers is inefficient. We consider the possible reasons for this experimental finding in the context of the orientational and structural properties of these systems.

## Experimental Section

**Multilayer Synthesis.** Metal–phosphonate multilayers were synthesized on polished Si(100) substrates (MultiCrystal Optics or Boston Piezo-Optics) having a native oxide layer of 5–20 Å, as determined by optical null ellipsometry. The substrates were cleaned immediately before use by immersion in piranha solution for 10 min (*Caution: Piranha solution is extremely corrosive and a strong oxidizer!*), rinsed with flowing distilled water, and dried with a N<sub>2</sub> stream. The surface was primed with a layer of 3-(aminopropyl)dimethylethoxysilane, by immersing overnight in a 0.5% v/v solution in toluene, followed by rinses with toluene, methanol, and water, and drying with N<sub>2</sub>. The resulting aminated surface was derivatized to the phosphonate in a solution that is 0.2 M in both POCl<sub>3</sub> and collidine in anhydrous acetonitrile for 10 min, then rinsed with acetonitrile and water. A layer of Zr<sup>4+</sup> was deposited onto the phosphorylated surface using a 5 mM ZrOCl<sub>2</sub> solution in 60% EtOH(aq) for 10 min. Multiple layers are synthesized through the alternate deposition of organobis(phosphonates) (at least 4 h deposition time) and Zr<sup>4+</sup> (10 min deposition time). The organobis(phosphonates) were dissolved in 80% DMSO, 18% EtOH, and 2% H<sub>2</sub>O solutions with 1 mM total concentration ([BDP] + [QDP] + [alkanebis(phosphonate)] = 1 mM). The syntheses of BDP, QDP, 1,6-hexanebis(phosphonate) (HBPA), and 1,12-dodecanebis(phosphonate) (DDBPA) have been reported previously.<sup>15,28</sup>

**Steady-State Optical Spectroscopy.** Absorbance spectra were recorded on a Hitachi U-4001 spectrophotometer with spectral resolution of 5 nm. Emission spectra were measured on a Hitachi F-4500 spectrometer. Slits were adjusted according to the emission intensity of the samples.

**Optical Null Ellipsometry.** The thicknesses of primed substrates and multilayer samples were determined using a commercial optical null ellipsometer (Rudolph Auto-El II) operating at 632.8 nm. Data were acquired and reduced using Rudolph software. For both primer and ZP layers, we used a value of the refractive index of  $n = 1.462 + 0i$  for the determination of film thickness.

**Fluorescence Lifetime Measurements.** Fluorescence lifetimes of chromophore-containing films were measured using time-correlated single photon counting (TCSPC). This system has been described in detail previously,<sup>30</sup> and we present only the essential details here. The second harmonic of the output of a mode-locked CW Nd:YAG laser (Quantronix 416) is used to pump a cavity-dumped dye laser (Coherent 702-2), operating at 630 nm (Kiton Red, Exciton). The output of the dye laser is frequency-doubled (LiIO<sub>3</sub> Type I SHG) to excite the multilayer samples at 315 nm. This wavelength is a maximum in BDP absorbance spectrum and, simultaneously, a minimum in the QDP absorbance spectrum. The sample surfaces are nearly parallel to the laser table and are held at ~5° with respect to the incident laser beam in two directions: toward the excitation beam and toward the detector. Fluorescence from the sample was imaged through a reflecting microscope objective and collected in two wavelength ranges with the detection bandwidth being set to 30 nm fwhm in each case. BDP emission was collected at 400 and 425 nm, and QDP emission was collected at 525 and 550 nm. Decays were measured at two wavelengths in each chromophore emission range to test for wavelength-dependent dynamics. None were found. As we had found in previous studies,<sup>28,29</sup> the recovered decay time constants were independent of collection wavelength, so the time constants reported for each chromophore are the averages of the lifetimes at both wavelengths in their respective emission range. The typical response function for this spectrometer is ~35 ps fwhm, as shown in Figure 1. The lifetimes we report are the results of fits of the data to the sum of two exponential decays using commercial software (Microcal Origin v. 5.0) and are reported as the average of the fits of at least three sets of experimental data in each wavelength range. The uncertainties represent the standard deviations of the average of the different sets of data.

(26) Horne, J. C.; Huang, Y.; Liu, G. Y.; Blanchard, G. J. *J. Am. Chem. Soc.* **1999**, *121*, 4419.

(27) Horne, J. C.; Blanchard, G. J.; LeGoff, E. *J. Am. Chem. Soc.* **1995**, *117*, 9551.

(28) Horne, J. C.; Blanchard, G. J. *J. Am. Chem. Soc.* **1996**, *118*, 12788.

(29) Horne, J. C.; Blanchard, G. J. *J. Am. Chem. Soc.* **1998**, *120*, 6336.

(30) DeWitt, L.; Blanchard, G. J.; LeGoff, E.; Benz, M. E.; Liao, J. H.; Kanatzidis, M. G. *J. Am. Chem. Soc.* **1993**, *115*, 12158.

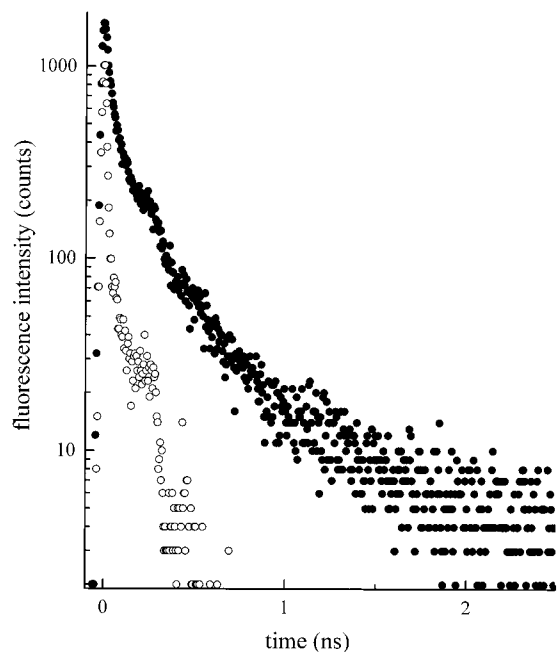


**Figure 1.** Typical instrument response function (○) and excited-state population decay (●) (425 nm) for a multilayer with full donor and acceptor layers. The emission at 425 nm is from BDP.

## Results and Discussion

The goal of this work is to understand the effects of chromophore orientation and layer structure on interlayer excitation transport behavior of oligothiophene chromophores in ZP multilayer structures. In the previous paper, we reported on photonic energy transfer within a single mixed chromophore layer.<sup>26</sup> For mixed D–A monolayers, we observed donor relaxation dynamics that were independent of acceptor concentration.<sup>26</sup> The absence of the expected concentration dependence was the result of structural heterogeneity within the layer. The experimental data are accounted for quantitatively by a model for excitation transport where  $\sim 100$  Å aggregated islands of chromophores are separated by distances sufficiently greater than 50 Å to preclude efficient inter-island excitation transport.<sup>29,31</sup> We turn our attention here to interlayer transport.

The TCSPC measurements yield a nonexponential decay for both donor and acceptor emission that is approximated well using a double-exponential decay function.<sup>26,31</sup> The short time component is  $\sim 200$  ps, which corresponds to that of radiative oligothiophene monomers, the same as seen in solution, and the long component has a time constant of  $\sim 1$  ns, which we consider to originate from radiative monomers in an aggregated chromophore environment.

The model for radiative dynamics of these layers has been developed by Song et al. for excitation transport in aggregated LB films of stilbazolium dyes.<sup>31</sup> The chromophores in a monolayer are present in two forms: most of the chromophores are in aggregates, with a smaller number present as monomers. In this model, the aggregate is excited, and it can either decay radiatively, a low probability event, or its excitation can be transferred to individual molecules in the aggregate. The excitation can “hop” randomly within the aggregate until it reaches a radiative monomer “defect” in the aggregate or one of the radiative, isolated chromophores nearby the aggregate. The different environments of the two radiative chromophores result

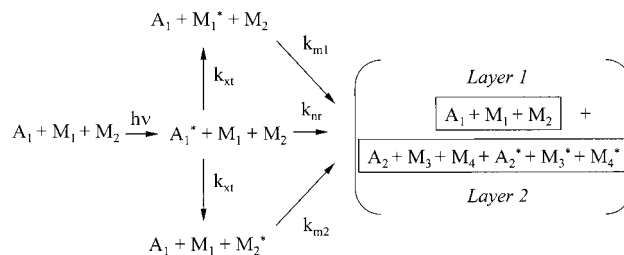


**Figure 2.** Kinetic scheme for population dynamics in layered structures.  $A_1$  is the donor aggregate, and  $A_2$  is the acceptor aggregate.  $M_1$  and  $M_2$  refer to radiative donor monomers, and  $M_3$  and  $M_4$  refer to radiative acceptor monomers. For a monolayer (*Layer 1*), only the species  $A_1$ ,  $M_1$ , and  $M_2$  are present in the relaxed system. For a multilayer (both *Layer 1* and *Layer 2*),  $A_2$ ,  $M_3$ , and  $M_4$  are also present in the relaxed system.

in the two fluorescence lifetimes, which provide the major contributions to the observed decay dynamics.

We present in Figure 2 the kinetic scheme relevant to this system. We have reported previously on this scheme for monolayers,<sup>26</sup> where *Layer 1* in Figure 2 is the final state. The difference between the monolayer case and that of multilayers lies in the presence of additional final states, containing  $A_2$ ,  $M_3$ , and  $M_4$ , where these species reside in layers adjacent to the initially excited layer. The only fundamental difference between the monolayer and multilayer systems will result from changes in  $k_{m1}$ ,  $k_{m2}$ , and  $k_{nr}$ . Our signal has significant contributions from each of these rate constants, and the Förster model predicts that  $k_{m1}$ ,  $k_{m2}$ , and  $k_{nr}$  depend sensitively on the presence or absence of *Layer 2*. The first questions must therefore be the applicability of the Förster model and the size of the expected changes in these rate constants resulting from the presence of acceptor layer(s).

The data presented in the previous paper demonstrate that dipolar energy transfer<sup>32,33</sup> within aggregates and between aggregates and monomers is operative. The photophysics that describe the behavior of the monolayers are also appropriate for multilayer systems. The existence of island structures within a given layer precludes efficient energy transfer over large distances within that layer. Because the growth of one layer on top of another requires spatial registration, donor and acceptor chromophores in adjacent layers will be in close spatial proximity to one another. We describe in Table 1 the multilayer structures we have synthesized to evaluate interlayer excitation transport.

For monolayers, the early time emission dynamics of the radiative monomers are mediated by diffusive excitation transport within the aggregate to the monomer.<sup>31</sup> This model provides exact agreement with atomic force microscopy data on the surface morphology of ZP monolayers.<sup>26</sup> This same physical picture holds for each layer in a multilayer assembly based on the form of our spectroscopic data (vide infra). The question at hand is to determine whether interlayer excitation transport can compete effectively with intralayer transport in ZP multilayers.

Dipolar excitation transport among like chromophores ( $D^* \rightarrow D$ ) as well as between donor and acceptor chromophores ( $D^* \rightarrow A$ ) can both proceed within a given layer.<sup>26</sup> The depopulation dynamics of  $D^*$  are related to the characteristic length scale of structural heterogeneity within the layer. For multilayers, our data point to the donor lifetime being dominated by intralayer

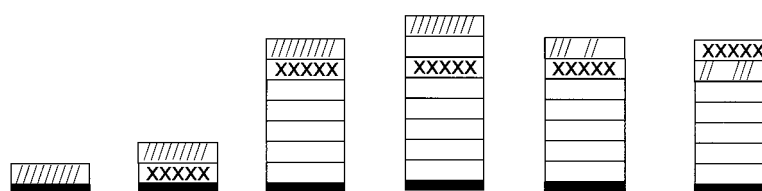
(31) Song, Q.; Bohn, P. W.; Blanchard, G. J. *J. Phys. Chem. B* **1997**, *101*, 8865.

(32) Förster, T. *Z. Naturforsch* **1949**, *A4*, 321.

(33) Förster, T. *Faraday Discuss. Chem. Soc.* **1959**, *27*, 7.

**Table 1.** Description of Layered Samples Corresponding to the Lifetime Data Presented in Figure 2

layer	Sample					
	1	2	3	4	5	6
8				100% BDP		
7			100% BDP	100% DDBPA	5% BDP; 95% HBPA	100% QDP
6			100% QDP	100% QDP	100% QDP	5% BDP; 95% HBPA
5			100% DDBPA	100% DDBPA	100% DDBPA	100% DDBPA
4			100% DDBPA	100% DDBPA	100% DDBPA	100% DDBPA
3			100% DDBPA	100% DDBPA	100% DDBPA	100% DDBPA
2		100% BDP	100% DDBPA	100% DDBPA	100% DDBPA	100% DDBPA
1	100% BDP	100% QDP	100% DDBPA	100% DDBPA	100% DDBPA	100% DDBPA



(D\*→D) excitation transport. Within the framework of the Förster model, this is an unexpected result. On the basis of what we know about the interface morphology, layered structure, and chemical composition, the only system property that can account for this finding is the presence of the metal–bis(phosphonate) layers. These polarizable, periodic structures appear to mediate interlayer excitation transport.

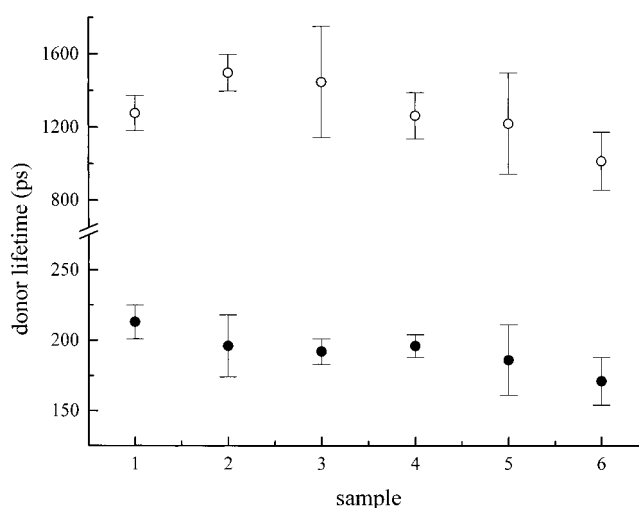
The Förster model can be used to describe both interlayer and intralayer relaxation processes. In either case, both spacing and donor orientation relative to the acceptor will determine the rate constant for energy transfer in the Förster model.<sup>32,33</sup>

$$k_{D-A} = \frac{3\kappa^2 R^6}{2\tau_D R_0^6} \quad (1)$$

The rate constant for energy transfer from donor to acceptor is  $k_{D-A}$ ,  $\tau_D$  is the excited donor radiative lifetime,  $R$  is the donor–acceptor distance, and  $R_0$  is the Förster critical radius, a term containing spectroscopic overlap and fluorescence quantum yield information. The term  $\kappa^2$  is a geometrical factor describing the relative orientation of donor and acceptor transition moments

$$\kappa = \sin \theta_D \sin \theta_A \cos \phi - 2 \cos \theta_D \cos \theta_A \quad (2)$$

where the angles  $\theta_D$  and  $\theta_A$  are the angles of the donor and acceptor with respect to the vector connecting them and  $\phi$  is the azimuthal angle between the transition moments. Angles of  $\theta_D = \theta_A = 90^\circ$  and  $\phi = 0^\circ$  correspond to a monolayer where the donor and acceptor are parallel to one another and perpendicular to the surface normal. For a multilayer where the donor and acceptor are stacked on top of one another,  $\theta_D = \theta_A = 0^\circ$  and the azimuthal angle  $\phi$  becomes coincident with the angles  $\theta$ . The terms  $\kappa^2$  and  $R$  are the experimental variables pertinent to the interpretation of our data.  $R_0$  and  $\tau_D$  are constants for the purposes of the experiments we report here. If interlayer transport competes effectively with intralayer transport, we expect the donor lifetime in a multilayer assembly to be sensitive to the distance between donor and acceptor layers. Experimen-

**Figure 3.** Fluorescence lifetimes measured for various layered systems. Decays were fit to the function  $f(t) = A_1 \exp(-t/\tau_1) + A_2 \exp(-t/\tau_2)$ .

tally, the lifetimes we measure for multilayers having adjacent donor–acceptor chromophore layers are the same as those we measure for individual chromophore layers (Figure 3). We observe that, for the layered oligothiophenes, interlayer Förster energy transfer does not compete efficiently with intralayer relaxation.

We attempt to understand these results in terms of the orientation and proximity of the donor and acceptor chromophore transition moments. The thiophene oligomers are a good choice for the investigation of energy transfer because of favorable spectroscopic properties. We calculate a value of  $R_0 = 57 \text{ \AA}$  for D\*→A transport and expect this quantity to be similar for D\*→D transfer. In either case, the relevant intermolecular distance lies within the critical radius,  $R_0$ , suggesting efficient interlayer and intralayer excitation transport.

The orientation of the donor and acceptor transition moments can also play an important role in determining the form of the

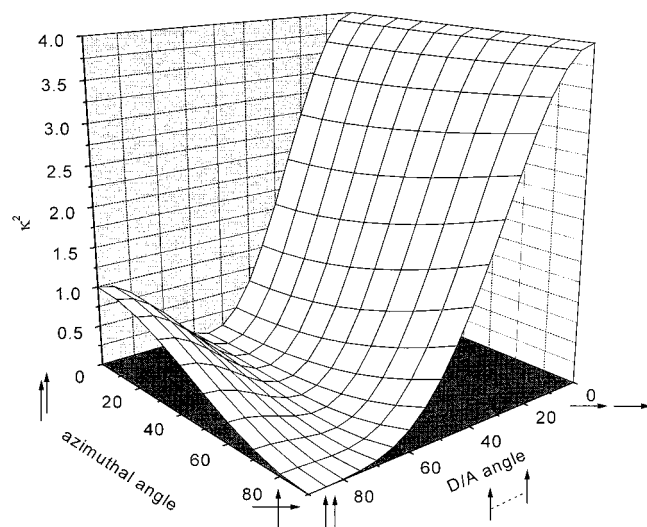


**Figure 4.** Calculated values of  $\kappa^2$  from eq 2 as a function of donor and acceptor orientation.

observed data, and this factor is accounted for in the Förster model through  $\kappa^2$ . The term  $\kappa^2$  can vary between 0 and 4 (eq 2 and Figure 4) depending on the relative orientation of the donor and acceptor transition moments. For isotropic systems and cases where orientational averaging occurs on a time scale that is fast relative to excitation transport,  $\langle \kappa^2 \rangle = 2/3$ . For interlayer transport, the value of  $\kappa^2$  can be significantly larger. If chromophores in the donor and acceptor layers are aligned with their transition moments both perpendicular to the layer plane, where  $\theta_D$  and  $\theta_A = 0^\circ$ ,  $\kappa^2 \sim 4$ , independent of  $\phi$ . In the limit of  $\theta_D$  and  $\theta_A = 0^\circ$ , the angle  $\phi$  becomes coincident with the angles  $\theta$  (eq 2 and Figure 4). The exact determination of intermolecular distance is not possible, owing to the delocalization of the molecular transition moments, but if we assume that  $R_{\text{interlayer}} \sim R_{\text{intra-layer}}$ , we will certainly be correct to within a factor of 2. For interlayer excitation transport, we expect several times greater efficiency than for intralayer transport, depending on the chromophore tilt angle within each layer. For ZP layers, we know from previous experiments that  $\theta \sim 30^\circ$  with respect to the surface normal.<sup>29</sup> Using this value for  $\theta_D$  and  $\theta_A$ , we recover  $\kappa^2 = 1.65$  for  $\phi = 0^\circ$  and  $\kappa^2 = 2.25$  for  $\phi = 90^\circ$  (see Figure 4). The dependence of  $\kappa^2$  on  $\phi$  is small for a tilt angle of  $30^\circ$ . For donor and acceptor tilt angles of  $\sim 30^\circ$ , interlayer transport is expected to be approximately twice as efficient as intralayer transport processes, assuming  $R_{\text{interlayer}} \sim R_{\text{intra-layer}}$ . This difference in efficiencies should be resolvable experimentally.

The fact that we do not observe interlayer excitation transport stands in sharp contrast to the predictions of the Förster model. This unexpected deviation from Förster behavior can be explained in the context of the structural properties intrinsic to the multilayer assembly. Dipolar excitation transport has been shown to explain our monolayer data quantitatively. We expect the Förster model to hold equally well for multilayers, as discussed above. An important assumption of the Förster treatment is that the dielectric response of the space between donor and acceptor is uniform. For the multilayer assemblies we have constructed, this assumption is not satisfied. Specifically, the layered structure of ZP films produces a spatial modulation of the dielectric response of the system. The presence of the Zr–bis(phosphonate) layer between donor and acceptor can, in principle, act to screen the oscillating transition dipole moment of the donor from the transition moment of the acceptor. The polarizable phosphonate anions can act as “polarizability screens”, precluding the efficient transfer of

excitation between individual layers. Although we are not aware of any direct measurements of the refractive index of bulk Zr–(PO<sub>3</sub>R)<sub>2</sub> compounds, where R is a simple substituent such as –H or –CH<sub>3</sub>, we estimate this value to be  $n \sim 1.65$ , and for organic layer constituents, we estimate  $n \sim 1.45$ . Regardless of the exact values, the modulation of  $n$  is experimentally seen to be sufficient to interfere with direct dipolar coupling of chromophore transition moments in adjacent layers.

While the screening of one transition moment from another is consistent with our experimental data, it is unfortunately not possible to acquire another body of data to evaluate this model directly. The nature of ZP multilayer chemistry does not allow variation of the multilayer structure in such a way as to preclude polarizability screening. Elimination or alteration of the Zr–bis(phosphonate) network will change the chemistry of the system and thus perturb the structural and spectroscopic properties of interest. Further experimentation using different interlayer linking chemistry, where the interlayer connections possess fewer polarizable functionalities, is underway in our laboratory. The scope and progress of this work is beyond what we can cover in this paper. We note that no apparent screening effect is seen in multilayer structures where the density and organization of polarizable moieties within the multilayer structure is limited.<sup>24</sup>

This is not the first work where interlayer transport phenomena have been observed, and it is instructive to consider the information available from these studies. Both Ungashe et al.<sup>13</sup> and Keller et al.<sup>34</sup> have examined photoinduced electron transport phenomena in layered materials containing alternating layers of (electron) donors and acceptors. The Bell Labs group used alternating layers of viologen and porphyrin phosphonates to show that the lifetime of the photoexcited porphyrin decreased in the presence of a viologen acceptor layer.<sup>13</sup> When the layers were separated by molecular spacers, the porphyrin lifetime increased. These findings were taken as evidence for interlayer photoinduced electron transport because there was no significant spectral overlap between the donor and acceptor, i.e.  $R_0 \sim 0$ . A fundamental difference between that work and ours is the extent of spectral overlap in our multilayers. Nonetheless, it is clear that interlayer transport phenomena can be seen in layered structures containing ZP functionalities.

The Mallouk group examined electron transport phenomena in multilayers grown by sequential adsorption of polyelectrolyte polymers.<sup>34</sup> In that work, different polymer layers containing redox-active species were exposed to a solution phase electron donor. The stepwise photoinduced, interlayer electron transport event required the presence of the solution phase electron donor to mediate the initial reduction of photoexcited Ru(II) to Ru(I). Only after this initial reduction was accomplished could direct interlayer electron transport proceed. The electrochemical pathway for \*Ru(II) oxidation and methylviologen reduction was not spontaneous in these multilayers. Perhaps of more significance to our work is their demonstration that the identity of the “sheets” separating the redox polymer layers can mediate the interlayer redox reaction substantially. Keller et al. showed that poly(styrenesulfonate) blocked interlayer electron transport while  $\alpha$ -ZrP allowed electron transport.<sup>34</sup> Our work on interlayer excitation transport indicates that ZP structures block photonic excitation transport. We do not consider that these two bodies of work are in conflict because of the fundamentally different nature of the transport phenomena in the two cases.

In addition to understanding interlayer photonic excitation transport, we can also add to our overall understanding of the

(34) Keller, S. W.; Johnson, S. A.; Brigham, E. S.; Yonemoto, E. H.; Mallouk, T. E. *J. Am. Chem. Soc.* **1995**, *117*, 12879.

morphology of the film as layers are built up. The priming chemistry and the chromophore aggregation give rise to island formation within a monolayer as reported previously, but there is some evidence in the literature that this structure is not preserved with the addition of multiple layers. One possibility for the growth of multiple layers is that one will grow in registration to another, preserving the initial island structure. This structural motif has been seen by AFM for two C<sub>16</sub>BPA layers.<sup>35</sup> It is also possible that the layers could “fan out” and grow together to form a more uniform surface with the addition of several layers. There is also some microscopic evidence for this process.<sup>36</sup> To address this question from a spectroscopic point of view, we synthesized films with chromophore layers that were spaced from the surface by five DDBPA layers, to probe the local structure further from the substrate. The optical response of the chromophore layers spaced away from the substrate is identical to that of monolayers formed directly above the substrate. This result points to the importance of chromophore aggregation coincident with the formation of the layers. Even if the films do “smooth out” as layers are added, we measure the same time constants for all cases, suggesting that the chromophores aggregate regardless of what type of surface they are deposited on. This finding suggests that the formation of statistically distributed chromophore layers will require a different chemical approach.

Another concern in the synthesis of chromophore-containing films is the effect of the surrounding dielectric environment on the optical properties and dynamic behavior of the chro-

mophores. In a film, a chromophore layer can be adjacent to several possible environments: the primed substrate, another chromophore layer, an alkane layer, or air. As shown in Table 1, we have varied both the donor and acceptor environments in the series of films we studied. In a previous study, we found that surrounding alkane layers had no effect on the dynamics of a single donor layer.<sup>28</sup> For the multilayer films we report on here, we find similar independence of the dynamics of both chromophores on the dielectric environment. This finding also points to the role of the polarizable ZP network between layers in restricting interlayer interaction in these MP films.

## Conclusions

We have found that excitation transport between layers of oligothiophene chromophores in a ZP multilayer structure does not compete efficiently with intralayer transport, in contrast to the predictions of the Förster model. The absence of interlayer excitation transfer can be accounted for by screening of adjacent chromophore layers by the Zr–bis(phosphonate) portion of layers. This screening is, in effect, the result of the spatial modulation of the nonresonant dielectric response of the system. These results are important for understanding the morphological, structural, and optical properties that will be useful for the incorporation of layered organic materials in future technologies.

**Acknowledgment.** We are grateful to the National Science Foundation for support of this work through Grant CHE 95-08763.

JA982552B

(35) Byrd, H.; Snover, J. L.; Thompson, M. E. *Langmuir* **1995**, *11*, 4449.

(36) Huang, Y.; Liu, G.-Y.; Horne, J. C.; Blanchard, G. J. In preparation.